

Mechanochemical Synthesis of LnCoO_3 (Ln: La, Pr, Dy)

O. Abe¹, N. Mantoku¹, T. Yamada² and S. Mitachi²

¹ The Research Center for Superplasticity, Ibaraki University, 4-12-1 Nakanarusawa, Hitachi 316-8511
Fax: +81 294 38 5078, e-mail: abe@mx.ibaraki.ac.jp

² Fine Ceramics Laboratory, Hokko Chemical Industry, 2165 Toda, Atsugi 243-0023
Fax: +81 46 230 2917, e-mail: mitachi-s@hokkochem.co.jp

Synthesis of lanthanoid cobaltates, LnCoO_3 (Ln: La, Pr, Dy), *via* the mechanochemically prepared complex (oxy-)hydroxides has been studied. The hydroxides are prepared by grinding Co(OH)_2 or Co_3O_4 with Ln_2O_3 (Ln: La, Dy) or Pr_6O_{11} in acetone containing a very small amount of H_2O in $\text{LnCoO}_3 \cdot 4\text{H}_2\text{O}$ composition. The starting hydroxides act as the reactive grinding aids to each other. La_2O_3 and Co(OH)_2 form the complex hydroxide, LaCo(OH)_5 , that is a sort of inorganic polymers having La-O-Co bond. The hydration affinity of trivalent Co^{3+} ions is not high enough to form complex hydroxide LaCo(OH)_6 . Then, the addition of H_2O_2 to the grinding liquid results in the formation of oxyhydroxide, LaCoO(OH)_4 . These (oxy-)hydroxides are directly converted to pseudo-tetragonal LaCoO_3 at 600°C and rhombohedral LaCoO_3 above 800°C without forming any by-product. The redox interaction between Co(OH)_2 and Pr_6O_{11} , which shows the poor reactivity with Fe_2O_3 , enables the formation of PrCoO(OH)_4 . Contrary, the reaction with Dy_2O_3 becomes poor.

Key words: LaCoO_3 , PrCoO_3 , DyCoO_3 , synthesis, mechanochemistry, crystallization

1. INTRODUCTION

Perovskite lanthanoid transition-metal oxides are candidate as redox catalysts and gas sensors, electrode materials for fuel cells, and so on [1,2]. These materials are synthesized by solid-state reactions and recently by build-up processes such as sol-gel methods. The authors have demonstrated the synthesis of perovskite- LnFeO_3 (Ln: La, Pr, Sm, Gd, Dy, and Yb) by a mechanochemical route in previous papers [3,4]. In this synthesis process, the starting Ln_2O_3 and Fe_2O_3 powders have been ground in organic liquids containing a small amount of H_2O , where Ln_2O_3 provides a Ln(OH)_3 colloids acting as a reactive grinding aid. The other starting material, Fe_2O_3 , is kneaded into the colloid to form complex oxyhydroxides. Slightly hydrated $\text{LnFeO}_3 \cdot x\text{H}_2\text{O}$ ($x=0.9-1.4$) has been obtained by the dehydration-condensation of the intermediate oxyhydroxide under the grinding stress.

In the present paper, this mechanochemical process has been applied to the synthesis of LnCoO_3 (Ln: La, Pr, Dy). The reactivity is discussed in relation to the potential of the starting materials to redox and hydration reactions in the combination of $\text{Co}^{\text{II}}\text{Co}^{\text{III}}_2\text{O}_4$ or $\text{Co}^{\text{II}}(\text{OH})_2$ and La_2O_3 , Pr_6O_{11} or Dy_2O_3 . The effect of H_2O_2 as an oxidant in the grinding liquid has also been studied.

2. EXPERIMENTAL

High-purity lanthanoid oxide powders (purity: >99.9%) supplied from Hokko Chem. Ind. were used after the heat-treatment at 500°C for 3h. The specific surface area (*SSA*) was 6.5 (La_2O_3), 2.2 (Pr_6O_{11}), and 1.6 $\text{m}^2 \cdot \text{g}^{-1}$ (Dy_2O_3). The cobalt source

used, Co_3O_4 and Co(OH)_2 , was the reagent-grade powders (Kanto-Kagaku). Mechanical grinding was conducted by the use of a planetary mill (Kurimoto-Tekko-Sho). Weighed mixture of the starting powders (20g as LnCoO_3) was encapsulated into the grinding vessel (capacity: 410 cm^3) made of stainless-steel with acetone (76 cm^3), a small portion of H_2O (equivalent amount to $\text{LnCoO}_3 \cdot 4\text{H}_2\text{O}$ composition including H_2O for Co(OH)_2), and grinding media ($\phi 2$, YTZ balls, fractional filling: 0.40). Grinding was performed for 3h with 15min cooling interval in every 1h to maintain the temperature below 50°C. The ground products were filtered with 0.2 μm Teflon membrane, washed with acetone, and dried at 85°C under vacuum. The ground products were calcined at 300-1000°C for 1h in air for crystallization.

Crystalline phases were identified by X-ray diffractometry (XRD, $\text{CuK}\alpha_1$, 40kV, 20mA) and X-ray photoelectron spectroscopy (XPS, $\text{MgK}\alpha$, 8kV, 30mA). Dehydration behavior of the ground products was examined by TG-DTA (10 $\text{K} \cdot \text{min}^{-1}$). Morphology was observed by scanning electron microscopy (SEM, Hitachi, S4300). *SSA* was determined by a N_2 -adsorption BET method.

3. RESULTS AND DISCUSSION

3.1 TG-DTA of the starting Co(OH)_2

Figure 1 shows the thermal decomposition behavior of Co(OH)_2 . The thermogravimetric curve indicated the mass loss at 200°C, 210-430°C and 930°C. The initial decomposition process at 200°C was the dehydration associated with the oxidation of Co^{II} . An exothermic peak was observed at 204°C

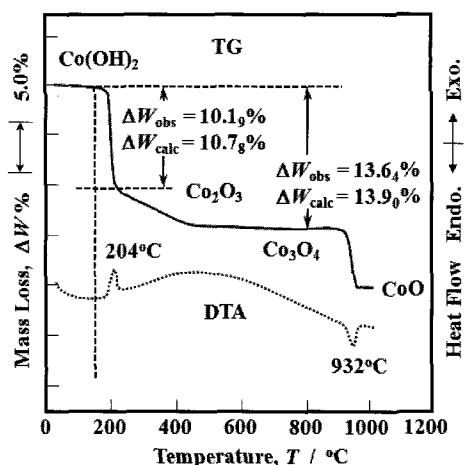
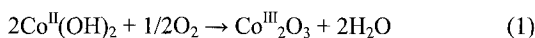
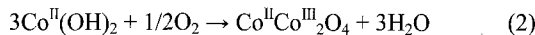


Fig. 1 TG-DTA curves of $\text{Co}(\text{OH})_2$.

and the determined mass loss ($\Delta W_{\text{obs}} = 10.1\%$) agreed with the calculation, 10.78% on reaction (1).



The Co_2O_3 formed was instable and decomposed to Co_3O_4 at $210\text{--}430^\circ\text{C}$. The ΔW_{obs} , 13.6% , was almost equal to 13.90% for reaction (2).



Co_3O_4 further decomposed to CoO above 930°C . This observation was referred to estimate the composition of the ground products.

3.2 Bond characteristics of the ground products

The XPS spectra of the ground products are shown in Fig. 2. For LC1 using Co_3O_4 , the $\text{La}3\text{d}$ peaks (844.2 and 848.1eV) and $\text{O}1\text{s}$ peak (534.2eV) were very close to those of $\text{La}(\text{OH})_3$, and the $\text{Co}2\text{p}$ peak was negligibly weak. This indicated the less interaction of Co_3O_4 and $\text{La}(\text{OH})_3$ and the surface of Co_3O_4 covered by $\text{La}(\text{OH})_3$. It was estimated that the pulverized Co_3O_4 was knead with the adhesive $\text{La}(\text{OH})_3$. The $\text{La}3\text{d}$ peak for LC2 and

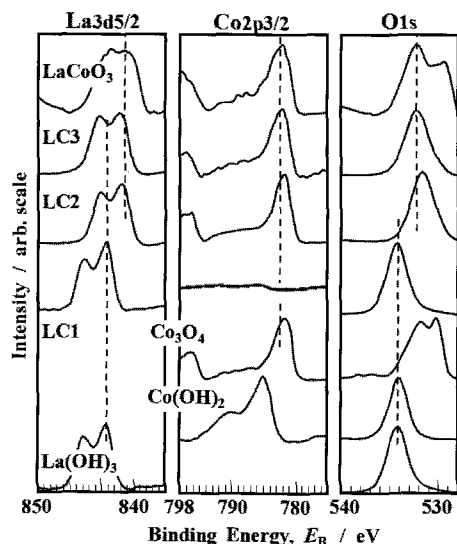


Fig. 2 XPS spectra of ground products.

LC3 appeared at 845.2 and 842.0eV , which were a little higher energy than those for LaCoO_3 . The $\text{Co}3\text{d}$ peak for LC2 and LC3 (782.1eV) was close to that of LaCoO_3 rather than $\text{Co}(\text{OH})_2$. The $\text{O}1\text{s}$ spectra also showed the E_B (531.7eV for LC2, 532.2eV for LC3) close to LaCoO_3 , $\text{Co}(\text{OH})_3$ and $\text{La}(\text{OH})_2$. However, the shoulder of $\text{O}1\text{s}$ spectrum for LaCoO_3 was not observed. Then, the hydrated LaCoO_3 , La_2Co -hydroxide, or La_2Co -oxyhydroxide were proposed as the structure of the ground products LC2 and LC3. The progress in reactions was suggested for LC3 because of the closer E_B of $\text{O}1\text{s}$ peak to LaCoO_3 .

The $\text{La}3\text{d}$ and $\text{O}1\text{s}$ XPS spectra for LC1 calcined at 400 and 700°C unchanged from those of the ground product, and the $\text{Co}2\text{p}$ peak started to appear at 400°C and increased at 700°C (Fig. 3). The $\text{La}3\text{d}$ and $\text{Co}2\text{p}$ spectra for LC2 and LC3 at 300°C unchanged from those of their ground products, but the $\text{O}1\text{s}$ spectrum for LC3 showed the shoulder similar to LaCoO_3 at $E_B = 530\text{eV}$. LaCoO_3 should form at the quite low-temperature of 300°C . At 1000°C , all the ground products showed the XPS spectra for LaCoO_3 .

3.3 Crystallization of the ground products

The estimation from XPS was ascertained by XRD. Figure 4 shows the XRD patterns of the ground and calcined LC1. As estimated from the XPS results, the ground product was the mixture of $\text{La}(\text{OH})_3$ and Co_3O_4 . $\text{La}(\text{OH})_3$ was dehydrated and crystallized to La_2O_3 at $600\text{--}700^\circ\text{C}$. The reflections of Co_3O_4 remained upto 700°C . However, the reflections for Co_3O_4 were evidently small against those of the mortar-mixed $\text{La}(\text{OH})_3\text{-}1/3\text{Co}_3\text{O}_4$, meaning the formation of the mixed hydroxide in part. The yield (ψ) of the ground product was evaluated to be 43% by comparing the peak intensity of $\text{La}(\text{OH})_3$ in LC1 to that of the mortar-mixed one. The ground products LC2 and

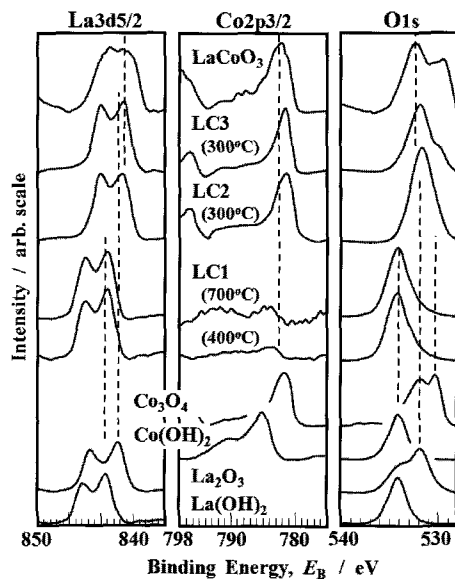


Fig. 3 Dependence of XPS spectra on calcination temp.

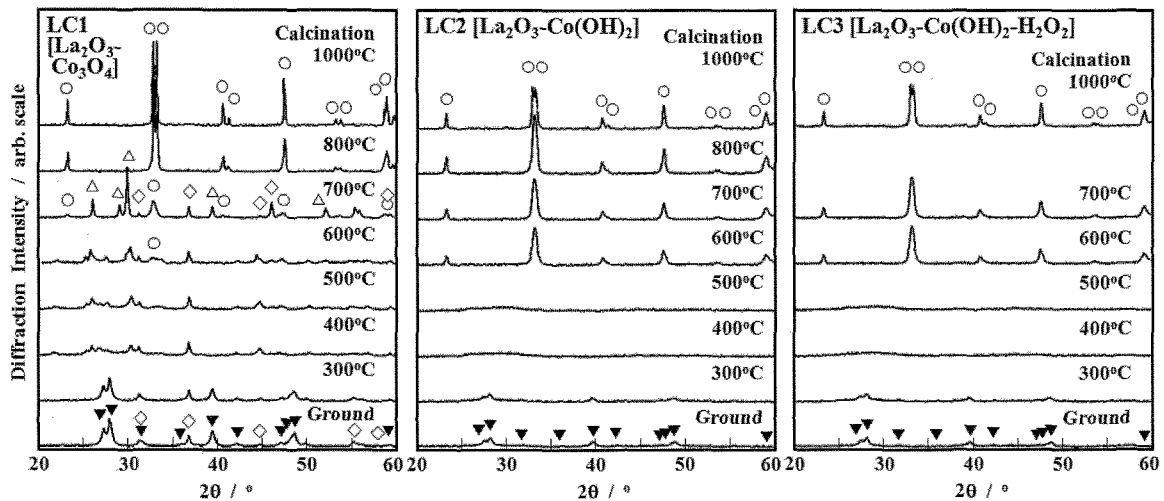
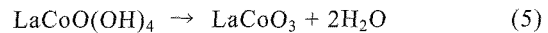
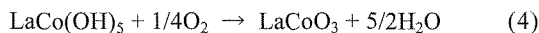
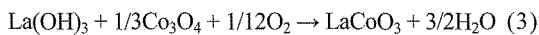


Fig. 4 XRD profiles of the ground products and calcined powders; ○: LaCoO_3 , ◇: Co_3O_4 , ▼: $\text{La}(\text{OH})_3$, △: La_2O_3 .

LC3 contains small amounts of $\text{La}(\text{OH})_3$. The yield (ψ) for LC2 and LC3 increased to 87% and 88%, respectively. The ground products were amorphous at 300-500°C, crystallized to pseudo-tetragonal LaCoO_3 at 600°C, and converted to rhombohedral phase above 800°C without forming any by-product. These observations were consistent with the discussion on XPS spectra.

3.4 TG-DTA of the ground products

Figure 5 shows the TG-DTA curves of LC1, LC2 and LC3. The ground product LC1 showed the mass loss at 400 and 700°C. The observed mass loss (ΔW_{obs}) at 100-1000°C was 10.36%, which agreed with 9.01% for the following reaction (3) when considering a little hydration of Co_3O_4 . The ground product LC2 and LC3 indicated ΔW_{obs} of 13.34% and 12.86% at 1000°C, respectively. These values agreed with ΔW_{calc} , 13.09% and 12.78%, for the reactions (4) and (5).



The DTA curve for LC2 indicated the exothermic peak for the oxidation of Co^{II} to Co^{III} at 170°C. However it was not observed for LC3. The hydrogen peroxide doped into the grinding liquid oxidized Co^{2+} to Co^{3+} with low hydration affinity, then, leads the formation of oxyhydroxide ($\Delta W_{\text{calc}} = 12.78\%$) rather than hydroxide. The $\text{LaCo}(\text{OH})_5$ (LC2) and $\text{LaCoO}(\text{OH})_4$ (LC3) formed amorphous LaCoO_3 at 400-600°C and crystallized at 641°C (LC2) and 609°C (LC3) with about 2% mass loss.

3.5 Synthesis of PrCoO_3 and DyCoO_3

This mechanochemical process was applied to the synthesis of PrCoO_3 and DyCoO_3 . Figure 6 shows the XRD patterns of the ground product and the calcined powders for $\text{Pr}_6\text{O}_{11}\text{-Co}(\text{OH})_2$ system without doping H_2O_2 . On the synthesis of praseodymium ferrite PrFeO_3 , Pr_6O_{11} , shows poor reactivity with $\text{FeO}(\text{OH})$ under grinding, and the XRD reflections of Pr_6O_{11} remained even at 700°C [3]. It was considered that the high stability

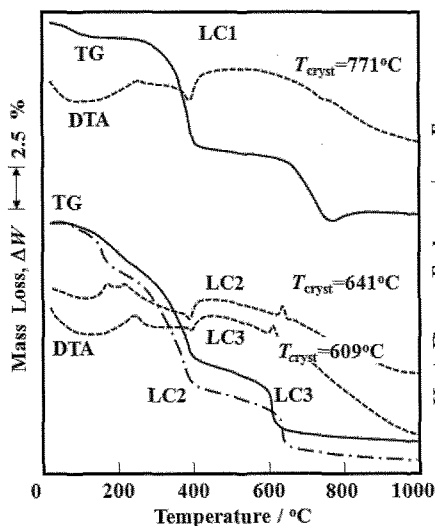


Fig. 5 TG-DTA curves of LC1, LC2 and LC3.

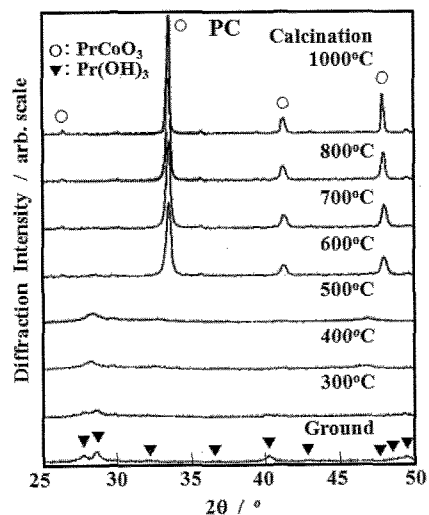
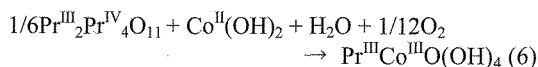


Fig. 6 XRD profiles for $\text{Pr}_6\text{O}_{11}\text{-Co}(\text{OH})_2$ system.

as oxide, that is the low affinity to hydration, of Pr^{IV} was the reason for the poor reactivity. So, when the Co^{II} can reduce the Pr^{IV} to Pr^{III} , there is a possibility to progress the formation of hydroxide or oxyhydroxide. The XRD patterns of the ground product PC indicated only the small reflections of $\text{Pr}(\text{OH})_3$ and no reflections from Pr_6O_{11} . The mass loss value ($\Delta W_{\text{obs}}=12.17\%$) was comparable to the calculated value ($\Delta W_{\text{calc}}=12.69\%$) for the oxyhydroxide, $\text{PrCoO}(\text{OH})_4$. The yield of $\text{PrCoO}(\text{OH})_4$ in the ground product (Ψ) was obtained to be 88% from the peak intensity of $\text{Pr}(\text{OH})_3$. The overall reaction can be represented as the following equation.



The small amount of O_2 required in (6) would be supplied from the ambient atmosphere under grinding or calcination. Tetragonal PrCoO_3 was successfully synthesized above 600°C .

Another example of the application was the synthesis of DyCoO_3 . The dysprosium ferrite, DyFeO_3 , is one of the most easily synthesized materials in the series of LnFeO_3 . However, contrary to the $\text{Pr}_6\text{O}_{11}\text{-Co}(\text{OH})_2$ system, the reactivity in $\text{Dy}_2\text{O}_3\text{-Co}(\text{OH})_2$ system markedly degraded. The reflections for Dy_2O_3 were observed in the grinding product and their intensity increased with the raise in temperature. The reason for the poor reactivity of DC was unclear; however, the addition of the oxidant should be needed.

3.6 Morphology of ground and calcined LC2, PC, DC

The SSA and morphology of the ground and calcined powders are cited in Table 1 and Fig. 8. The SSA of the ground products decreased with the increase in reactivity except DC. The SEM photographs in Fig. 8 showed the agglomeration. This was strongly related to the mechanism expected, where the adhesive $\text{Ln}(\text{OH})_3$ colloids were used as the reactive grinding aid.

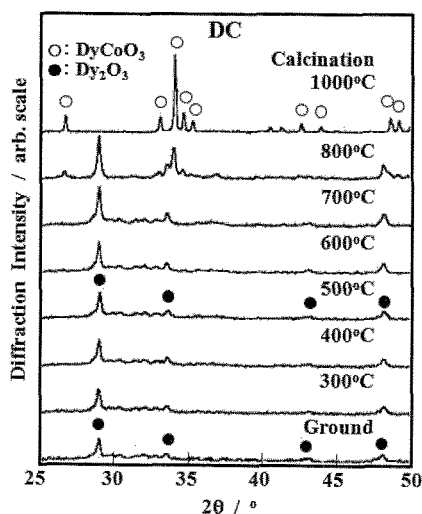


Fig. 7 XRD profiles for $\text{Dy}_2\text{O}_3\text{-Co}(\text{OH})_2$ system.

Table 1. Specific surface area (SSA) of the ground and calcined powders

	Ground	Calcined powder			
		400°C	700°C	800°C	1000°C
LC1	47.5	42.8	6.9	5.3	—
LC2	23.9	13.2	3.9	—	1.4
LC3	17.9	11.4	6.9	5.1	—
PC	12.2	10.2	3.0	—	1.7
DC	11.7	8.7	5.2	—	1.3

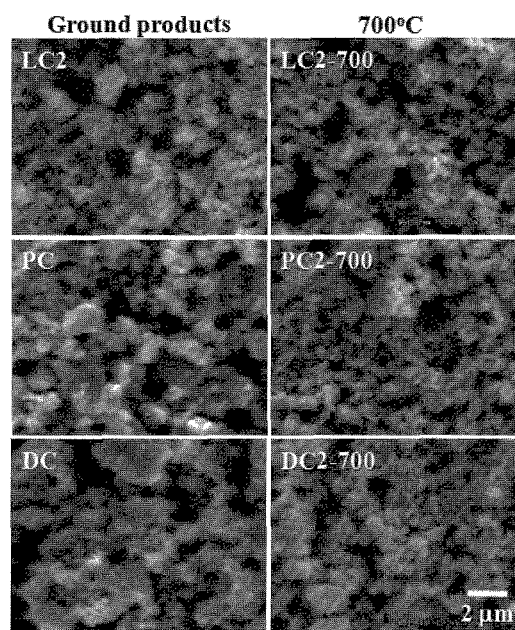


Fig. 8 Morphology of ground products.

4. CONCLUSION

The mechanochemical process is successfully applied to the synthesis of LaCoO_3 . The ground products obtained from La_2O_3 and $\text{Co}(\text{OH})_2$ are amorphous complex hydroxide and converted to pseudo-tetragonal LaCoO_3 at 600°C and rhombohedral one above 800°C . The addition of H_2O_2 to the grinding liquid results in the oxidation of Co^{II} to Co^{III} to contribute the formation of oxyhydroxide, $\text{LaCoO}(\text{OH})_4$, which can be dehydrated to amorphous LaCoO_3 at 300°C . The reduction activity of $\text{Co}^{\text{II}}(\text{OH})_2$ enables the formation of PrCoO_3 from Pr_6O_{11} , but makes the synthesis of DyCoO_3 difficult.

References

- [1] S. Kaliaguine, A. Van Neste, V. Szabo, J. E. Gallot, M. Bassir and R. Muzychuk, *Applied Catalysis A: General*, **209**, 345 (2001).
- [2] M. Popa, J. Frantti, M. Kakihana, *Solid State Ionics*, **154-155**, 135 (2002)
- [3] O. Abe, N. Mantoku, T. Yamada, S. Mitachi, *Trans. Mater. Res. Soc., Jpn.*, **32**, 123 (2007).
- [4] O. Abe, N. Mantoku and S. Mitachi, *Proc. Int'l. Symp. on Synergistic Effects of Mater. and Processing*, Kumamoto, Japan (2006) pp.7-10.
- [5] M. Koike and O. Abe, *Solid State Ionics*, **172**, 217 (2004).
- [6] O. Abe, M. Koike and R. Umezawa, *J. Powder Technol. Jpn.*, **42**, 199 (2005).